

PAPER • OPEN ACCESS

Finite element simulations of the bending resistance of square profiles with topological modifications

To cite this article: Q Estrada *et al* 2019 *IOP Conf. Ser.: Mater. Sci. Eng.* **710** 012031

View the [article online](#) for updates and enhancements.

Finite element simulations of the bending resistance of square profiles with topological modifications

Q Estrada¹, D Szwedowicz², J Vergara-Vazquez², A Rodriguez-Mendez³, J Silva-Aceves¹ and L C Wiebe¹

¹ Universidad Autónoma de Ciudad Juárez (UACJ), Instituto de Ingeniería y Tecnología, Ciudad Juárez, Chihuahua, México

² Centro Nacional de Investigación y Desarrollo Tecnológico TecNM/Cenidet, Departamento de Ingeniería Mecánica, Cuernavaca, Morelos, Mexico

³ University of California, Department of Mechanical Engineering, CA., USA

quirino.estrada@uacj.mx

Abstract. Bending resistance is one of the most important requirements in automobile structural members when lateral crashes occur. For this purpose, the current paper studies the bending and crashworthiness capacity of square profiles with topological modifications. Several finite element simulations were carried out using Abaqus/Explicit software. The topological modifications consisted in combining a square cross-section with polygonal and circular simple cross-sections. In all cases, the profiles evaluated were simulated with mechanical properties for aluminium alloy 6063-T5 with the same mass. The feasibility of our numerical study was validated by a three-point bending tests of a square tube using a Shimadzu universal test machine. Additional to the assessment of complex cross-sections, numerical results for simple cross-sections are presented. A better crashworthiness performance is obtained when the square section of a simple profile is reinforced with topological modifications. According to the simulation results, a complex cross-section can improve the crushing force efficiency up to 77.9% with respect to a single square profile. Regarding cross-sections with topological modifications, the best bending resistance and energy absorption capacity is obtained when the square section is combined with a square profile. This means an increase of 9.2 % of energy absorption (E_a) and 5.67% of CFE respect to the cross-section formed by square and triangular shapes.

1. Introduction

Safety of the passengers is one of the most important requirements when a new vehicle is designed. This priority is based on the annual deaths related to car crashes around the world [1,2]. Mexico is ranked in the ninth place of countries with the highest number of deaths. In this sense, 17,000 Mexican deaths associated with traffic accidents were reported in 2017 [3]. To counter these fatalities, the design of structural members considering the concept of crashworthiness is the fundamental target recognised by automobile manufacturers [4,5]. Crashworthiness refers to the ability of a structure to absorb a large amount of energy by plastic deformation and to minimise the injuries of the passenger during car collisions [6,7]. Thin-walled structures are widely used as crash boxes in frontal collisions or side-impact beams in lateral collisions [8]. Many parameters influence the energy absorption capacity of the thin-walled structures [9,10]. However, the cross-section is among the most important parameters and thus it is considered for topological studies [11,12]. Focusing on lateral crashes, an optimal design of the cross-section can reduce the mass of the components without sacrificing the strength and safety



requirements. In this context, Tang et al. [13] carried out a numerical study of thin-walled structures with various cross-sections subjected to lateral impacts. In this study, simple geometries and composite complex profiles were evaluated by dynamic three-point bending tests. Complex profiles involve the combination of single profiles such as a circle, square, hat, ellipse and trapezoid profiles. According to the results, the use of complex cross-sections increases the crush force efficiency (CFE) by up to 0.87 relative to simple shapes. Wang [14] performed a numerical study of the bending resistance of multi-cell square arrangements by a three-point bending test. For this purpose, the square cross-section of simple profiles was reinforced by longitudinal and transversal plates. It was concluded that more partition plates do not directly translate improvement in the energy absorption capacity. However, this is strongly dependent on the relative position of the punch and partition plates. On the other hand, a similar behaviour was obtained by analysing aluminium circular profiles with stiffeners [15]. Special emphasis was set on the effect of damage evolution model on the energy absorption E_a . A better performance was obtained when the circular cross-section was reinforced in the longitudinal and transversal direction by 4 plates. A CFE value of 0.85 was obtained, which means an improvement of the energy absorption capacity of 34% relative to a single circular profile. In [16] a topological investigation of several profiles subjected to bending loads was carried out. In this study, single and multi-cell structures with triangular, square, hexagonal and circular shapes were numerically evaluated by a three-point bending test. According to their results, relative to single profiles, the effectiveness of multi-cell structures to improve the energy absorption performance was observed. After several simulations, the authors concluded that the best bending performance was for circular multi-cell structures with a CFE equal to 0.88. Lastly, many studies have been conducted in order to obtain the best cross-sectional shape. However, for the specific case of square profiles, it has been barely reported.

Thus, in the present article, a topological study of square thin-walled structures under bending load was performed numerically using Abaqus/Explicit FEM software. From a square base cross-section, several new complex cross-sections were proposed. In this sense, polygonal and circular shapes were combined with the square cross-section. The evaluation of the single and complex profiles was carried out by a three-point bending test.

1.1. Theoretical bending collapse for single square profiles

The bending resistance and energy absorption capacity of square profiles are directly influenced by the bending collapsed mode [17,18]. A torsional moment (M) at the end of the profile generates the formation of a central hinge line. This induces an inward fold at the compression flange [19]. As the inward fold gets deeper, new travel hinge lines GA , EA , KA and LA are formed. From these travel lines two outward folds at the adjacent flanges are formed (see figure 1).

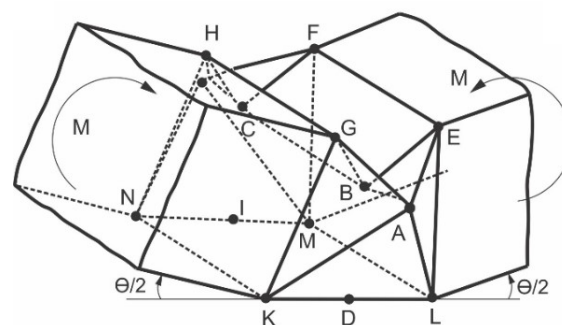


Figure 1. Theoretical bending collapse mode for a single square profile [19].

1.2. Energy absorption parameters

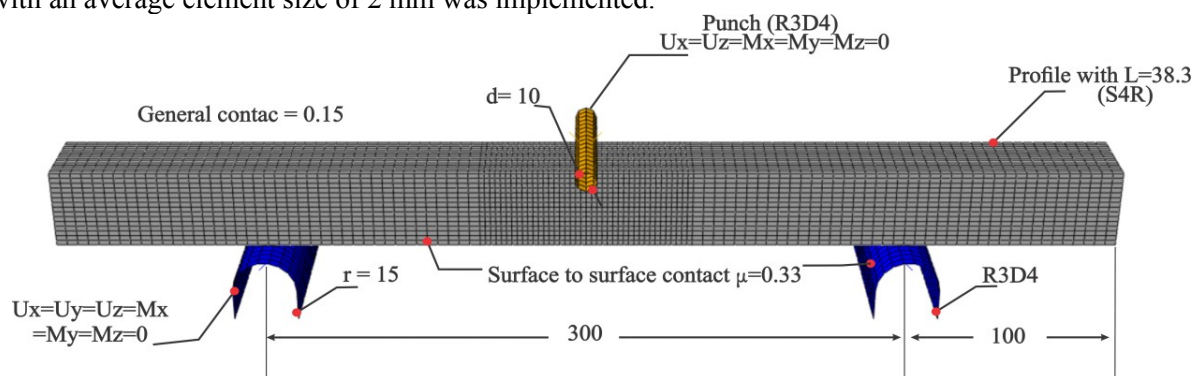
The assessment of simple and complex profiles regardless of manufacturing material can be carried out by dimensional and dimensionless parameters. In this way, the parameters listed in table 1 are obtained/calculated from bending force (F) versus displacement (δ) curves [20].

Table 1. Energy absorption parameters.

Peak load [P_{max}] kN	Mean Force [P_m] kN	Energy absorbed [E_a] kJ	Crush force efficiency [CFE]	Specific energy absorption [SEA]
Obtained from curve	$P_m = \frac{E_a}{\delta}$	$E_a = \int_0^{\delta} F. d\delta$	$CFE = \frac{P_m}{P_{max}}$	$SEA = \frac{E_a}{m}$

2. Validation of the three-point bending test model

To validate the feasibility of our numerical techniques, a square thin-walled profile was numerically and experimentally investigated in a three-point bending test (see figure 2). The discrete model was developed in Abaqus/explicit. The square profile has a side width (W) of 38.5 mm, length of 250 mm and thickness of 1.40 mm. The tube was modelled using shell elements (S4R) with elastoplastic properties for aluminium 6063-T5 alloy. An elastic modulus of $E=66,940$ MPa, Poisson coefficient (ν) of 0.33, yield stress (σ_y) of 158.78 MPa and density of 2700 kg/m³ were used. On the other hand, pin supports and a punch were modelled as rigid bodies with R3D4 elements. As boundaries conditions, the punch was unconstrained only in the y -direction to allow the bending process at 6 mm/min. During the contact interaction, a friction coefficient of 0.3 was used. Lastly, from a convergence analysis, a mesh with an average element size of 2 mm was implemented.

**Figure 2.** Discrete model of the three-point bending test of a square profile.

The numerical and experimental results are presented in figure 3. As expected, the square profile presented a typical bending force v displacement curve which is characterised by an initial maximum peak load (6 kN) followed by a drop of the bending force (see figure 3a). A good agreement between both models was calculated with differences in the order of 2%. On the other hand, to make a qualitative comparison of the bending collapse mode, it is observed that the discrete model captures correctly the deformation mode (see figure 3b). Thus, the discrete model is validated, and thus we continue with the topological studies of square profiles by numerical simulations.

3. Numerical topological study

In this study, a topological analysis of square profiles under bending load using Abaqus/explicit was conducted. The evaluated profiles were obtained by combining a square with polygonal and circular cross-sections. In order to obtain a comparison pattern, the study of single square profiles is also reported. In all cases, the thin-walled structures were made with aluminium alloy 6063-T5 and were evaluated by a quasi-static three-point bending test. Details of the evaluated profiles are displayed in table 2.

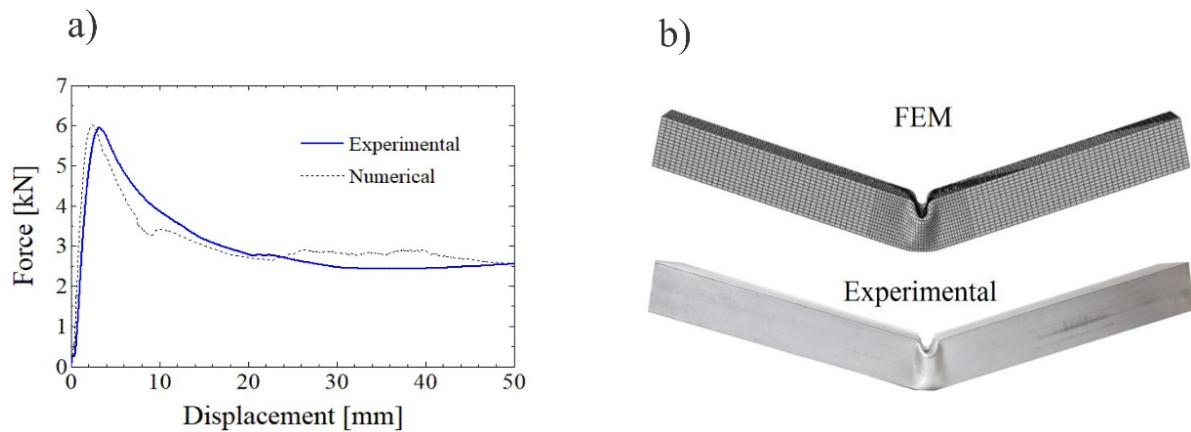


Figure 3. a) Force v displacement response of a square profile, and b) final deformation mode.

Table 2. Evaluated profiles with complex cross-sections, units in mm.

Specimen code	Geometrical base	Thickness [mm]	Length [mm]	Mass [kg]
SQ	Square	1.4	500	0.290
ST	Square, triangle	0.819	500	0.290
SS-A	Square, square	0.826	500	0.290
SS-B	Square, square	0.867	500	0.290
SH-A	Square, hexagonal	0.85	500	0.290
SH-B	Square, hexagonal	0.85	500	0.290
SC	Square, circular	0.853	500	0.290

4. Results and discussion

The bending and energy absorption performance of the evaluated structures was obtained by the study of force versus displacement curves. The curves show qualitative similarities with the curve for a typical square profile, which is characterised by an initial P_{max} at the bending process with a subsequent drop of force. However, the transition of P_{max} to P_m for complex profiles was smoothed. The opposite case is observed for the typical square profile where an abrupt drop of bending force is observed. According to Figure 4, as the number of edges of the internal cross-section increases, a convergence of the mechanical behaviour is observed. In this way, profiles with hexagonal (SH-A and SH-B) and circular (SC) reinforcement cross-section presented a similar bending response. Regarding the P_{max} value, in all

cases, the complex profiles presented lower P_{max} values than a typical profile (SQ). In this sense, P_{max} values in a range of 4.2 kN to 4.5 kN were obtained.

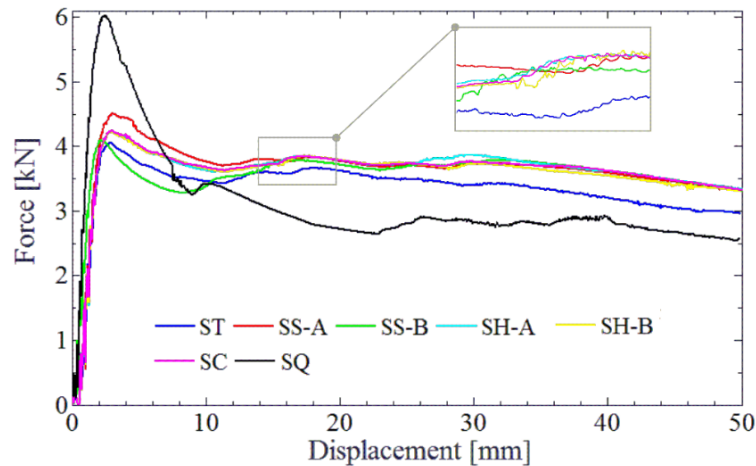


Figure 4. Force vs. displacement curves for the evaluated profiles.

From the area under the load v displacement curve, the energy absorption, including elastic and plastic deformation, is obtained (see figure 5). Three trends were clearly observed. As expected, the poorest performance was achieved for the single profile (SQ). Meanwhile, a reasonable performance was obtained by using a triangular reinforcement cross-section (ST). A third category is formed when the internal cross-section has an edge number equal to four or higher. For this group, similar energy absorption capacities are obtained in the order of 180 J. However, zooming at 50 mm of displacement, the importance of the topological analysis is visible. In this way, a greater number of edges contributed to a better stability of the structure. Thus, higher energy absorption was computed.

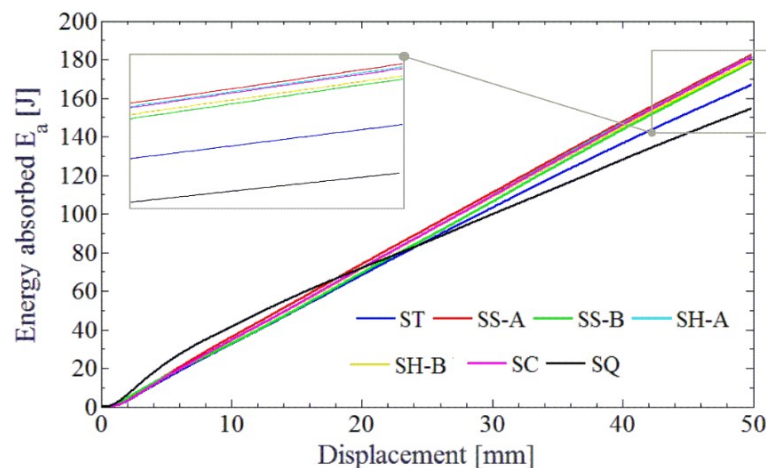


Figure 5. Comparison of energy absorption for the evaluated profiles.

Despite having the same mass, all complex cross-sections increased the stiffness of the square profile. Thus, the theoretical deformation mode, presented in figure 1, was modified. The final bending deformation at 50 mm is presented in Tables 3-4. From the cross-section cut view, as the reinforced internal profile tends to a circular shape, more advantageous plastic deformation is obtained. The opposite case was observed for the ST (triangular base) arrangement.

Table 3. Final deformation state for the evaluated complex arrangements.

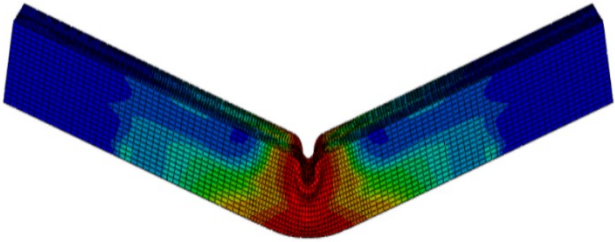
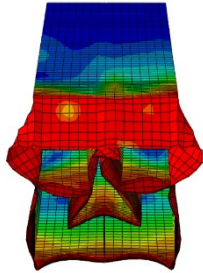
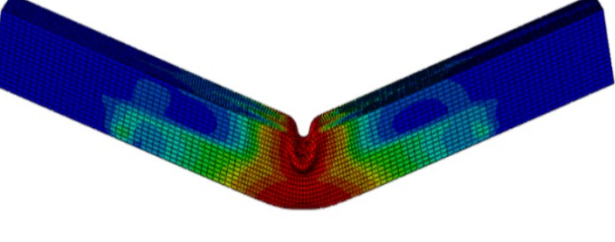
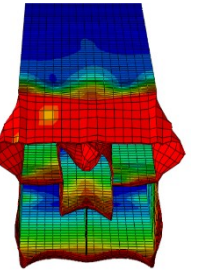
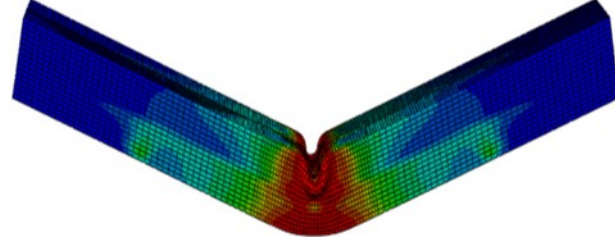
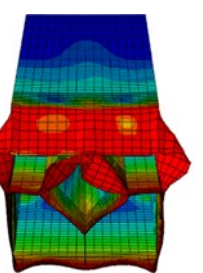
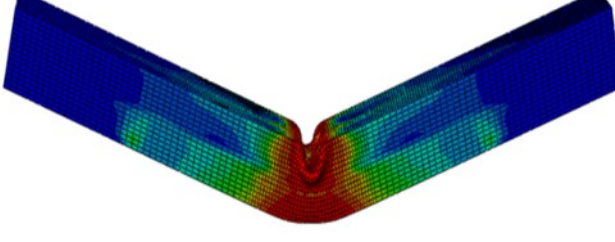
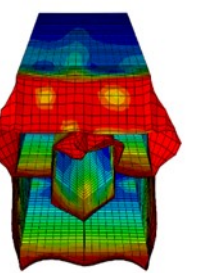
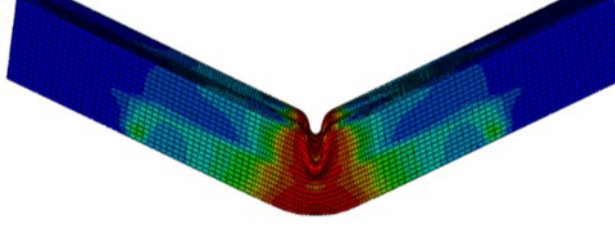
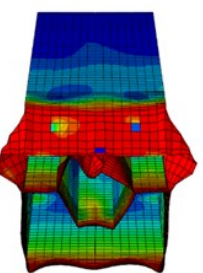
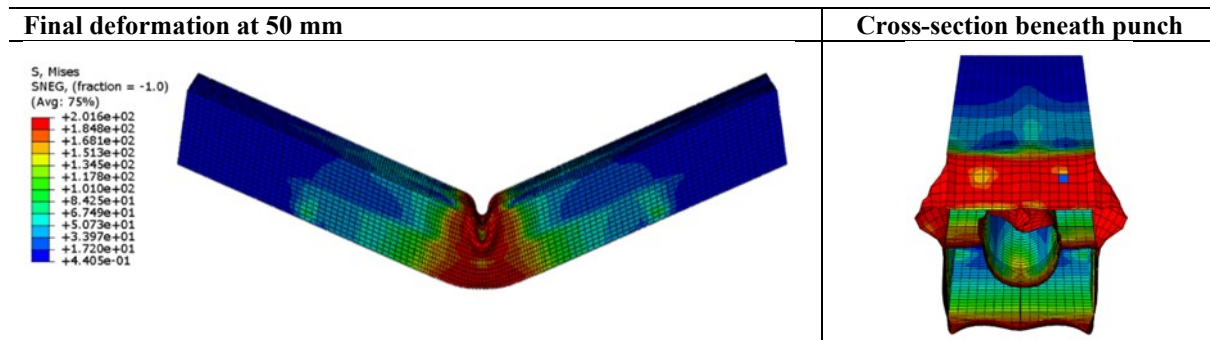
Final deformation at 50 mm	Cross-section beneath punch
<p>S, Mises SNEG, (fraction = -1.0) (Avg: 75%)</p>  <p> +2.016e+02 +1.848e+02 +1.680e+02 +1.513e+02 +1.345e+02 +1.177e+02 +1.010e+02 +8.419e+01 +6.743e+01 +5.065e+01 +3.389e+01 +1.711e+01 +3.402e-01 </p>	
<p>S, Mises SNEG, (fraction = -1.0) (Avg: 75%)</p>  <p> +2.016e+02 +1.848e+02 +1.680e+02 +1.512e+02 +1.344e+02 +1.176e+02 +1.008e+02 +8.404e+01 +6.725e+01 +5.046e+01 +3.366e+01 +1.687e+01 +7.982e-02 </p>	
<p>S, Mises SNEG, (fraction = -1.0) (Avg: 75%)</p>  <p> +2.016e+02 +1.848e+02 +1.681e+02 +1.513e+02 +1.345e+02 +1.177e+02 +1.010e+02 +8.420e+01 +6.743e+01 +5.066e+01 +3.389e+01 +1.712e+01 +3.535e-01 </p>	
<p>S, Mises SNEG, (fraction = -1.0) (Avg: 75%)</p>  <p> +2.016e+02 +1.849e+02 +1.681e+02 +1.514e+02 +1.347e+02 +1.179e+02 +1.012e+02 +8.448e+01 +6.775e+01 +5.102e+01 +3.429e+01 +1.756e+01 +8.246e-01 </p>	
<p>S, Mises SNEG, (fraction = -1.0) (Avg: 75%)</p>  <p> +2.016e+02 +1.848e+02 +1.681e+02 +1.513e+02 +1.345e+02 +1.177e+02 +1.010e+02 +8.421e+01 +6.745e+01 +5.068e+01 +3.391e+01 +1.714e+01 +3.729e-01 </p>	

Table 4. Final deformation state for the SC profile.

The assessment of the complex and single profile was carried out with the crashworthiness parameters showed in table 1. As a result, a summary of the results is presented in Table 5. Complex profiles allowed a decrease of peak load (P_{max}) in the range from 25.77% to 33.34% with respect to a single profile (SQ). The lowest P_{max} value equal to 4.06 kN was computed by the ST arrangement, and the highest, by the square profile with internal square reinforced, at 45° (SS-B). The effectiveness of the complex profile was demonstrated by calculating the energy absorption (E_a). An improvement of E_a capacity up to 21.34% was achieved by the SS-B profile. The highest values for mean force (P_m) and specific energy absorption (SEA) were 3.65 kN and 0.629 J/g, respectively. Despite obtaining the poorest E_a performance, the profile with triangular reinforcement (ST) presented an increase of 11.01% relative to the SQ profile. The poorest behaviour is attributed to the instability of the triangular shape during the bending process. According to our numerical results, it was determined that the E_a capacity of the structure is primarily dependent on the location of the internal profile followed by the cross-sectional shape. This explains the differences found for arrangements with denomination A and B, which have the same internal cross-section but at different positions.

Table 5. Summary of numerical results.

Code	P_{max} [kN]	P_m [kN]	E_a [J]	SEA [J/g]	CFE
SQ	6.09	3.01	150.42	0.518	0.4900
ST	4.06	3.34	166.99	0.575	0.8233
SS-A	4.10	3.57	178.64	0.616	0.8720
SS-B	4.52	3.65	182.52	0.629	0.8071
SH-A	4.25	3.63	181.75	0.627	0.8548
SH-B	4.23	3.58	179.44	0.618	0.8480
SC	4.25	3.62	181.33	0.625	0.8526

Energy absorption and peak load parameters are fundamental crashworthiness indicators. However, the optimal performance of the structure is obtained when the crush force efficiency (CFE) tends to unity. This means that a higher E_a value does not always represent the best crashworthiness behaviour. The best CFE performance was obtained for the SS-A structure, with 0.8720. In this way, a square internal reinforcement increased the stability of the structure during the bending process. Thus, better stress distribution was achieved. Additionally, the position of the internal square profile allowed a greater plastic deformation. Finally, from our numerical findings, the use of square reinforcement increases the crashworthiness capacity of square profiles. Thus, this kind of structure is highly recommendable to counter the harmful effects of lateral crashes.

5. Conclusions

A numerical study of crashworthiness and bending performance of square profiles with topological modifications was carried out. According to our study, the following conclusions were found.

1. Using the same mass value (0.29 kg), all proposed complex profiles showed a better energy absorption performance compared to a single square profile. An improvement in the range from 21.34 to 11.01% was computed.
2. The internal reinforcement cross-section plays an important role in the crashworthiness capacity of complex profiles. Polygonal cross-section with four or more edges presents a higher stability of the structure. Thus, the formation of travel and hinge plastic lines required greater external work.
3. Although the internal cross-section affects the crashworthiness performance of the structure, the position of the internal profile becomes more important. To compare complex profiles with a similar internal cross-section i.e SS-A, SS-B, SH-A, SH-B, a better performance was obtained when the load is transferred directly to the horizontal edge. In this way for equal internal cross-sections, differences of CFE between 0.80% and 7.44% were computed.
4. The best crashworthiness performance was obtained by a square profile with an internal square tube (SS-A). In this way, an increase of 21.34% and 77.9% for SEA and CFE were achieved. Therefore, this topology is an effective and low-cost alternative to decrease the injuries and fatalities during lateral car crashes.

6. References

- [1] WHO 2019 *Global status report on road safety 2018* Available from: https://www.who.int/violence_injury_prevention/road_safety_status/2018/en/
- [2] Nagel G M and Thambiratnam D P 2006 *Int. J. Impact. Eng.* **32(10)** 1595-620
- [3] CONAPRA 2018 *Informe sobre la situación de la seguridad vial, México 2017*. Secretaria de Salud. Available from http://mapasin.org/wp-content/uploads/2018/10/Informe_SV_2017.pdf
- [4] Tran T, Le D, and Baroutaji A. 2019 *Eng. Struct.* **182** 39-50
- [5] Huang J P, and Liu R Q. 2018 *IOP Confer, ser. Mater.Sci.Eng.* **382(4)** 042012
- [6] Lukaszewicz, D. H.-J. A 2013 Automotive Composite Structures for Crashworthiness. *In Advanced Composite Materials for Automotive Applications* ed. John Wiley & Sons Ltd (Chichester, UK) p 99–127
- [7] Lozzi, A. 1981 *Int. J. Veh. Design.* **2(4)** 470-79
- [8] Baroutaji A, Sajjia M, and Olabi A G. 2017 *Thin-Walled Struct.* **118** 137-63
- [9] Huang Z, and Zhang X. 2019 *Thin-Walled Struct* **137** 231-50
- [10] Huang Z, and Zhang, X. 2018 *Int. J. Mech. Sci.* **144** 461-79
- [11] Li Z and Lu F 2015 *J Reinf Plast Comp.* **34(9)** 761–68
- [12] Yin H, Xiao Y, Wen G, Qing Q, and Deng Y. 2015 *Thin-Walled Struct.* **94**, 1-12
- [13] Tang T, Zhang W, Yin H and Wang H 2016 *Thin-Walled Struct.* **102** 43–57
- [14] Wang Z, Li Z and Zhang X 2016 *Thin-Walled* **107** 287–99
- [15] Estrada Q, Szwedowicz D, Gutierrez-Wing E, Silva-Aceves J, Rodriguez-Mendez A, Elias-Espinosa M and Bedolla-Hernandez J 2019 *P. I. Mech. Eng. D-J Aut.* **233(8)** 2120–38
- [16] Estrada Q, Szwedowicz D, Rodriguez-Mendez A, Silva-Aceves J, Wiebe L C, Castro J S, Castillo S A 2019 *MATEC Web of Conferences* **252** 07005
- [17] Kecman D. 1983 *Int. J. Mech. Sci.* **25(9-10)** 623-36
- [18] Elchalakani M, Zhao X L, and Grzebieta R H. 2002 *Int. J. Mech. Sci.* **44(6)** 1117-43
- [19] Santosa S, Banhart J and Wierzbicki T 2001 *Acta Mech.* **148(1-4)** 199–213
- [20] Sun G, Tian X, Fang J, Xu F, Li G, and Huang X. 2015 *Int. J. Impact. Eng.* **78** 128-37.